Cell Reports, Volume *37*

Supplemental information

Single-cell analysis of COVID-19, sepsis, and HIV infection reveals hyperinflammatory and immunosuppressive signatures in monocytes

Nianping Liu, Chen Jiang, Pengfei Cai, Zhuoqiao Shen, Wujianan Sun, Hao Xu, Minghao Fang, Xinfeng Yao, Lin Zhu, Xuyuan Gao, Jingwen Fang, Jun Lin, Chuang Guo, and Kun Qu

Supplemental Figures and Legends

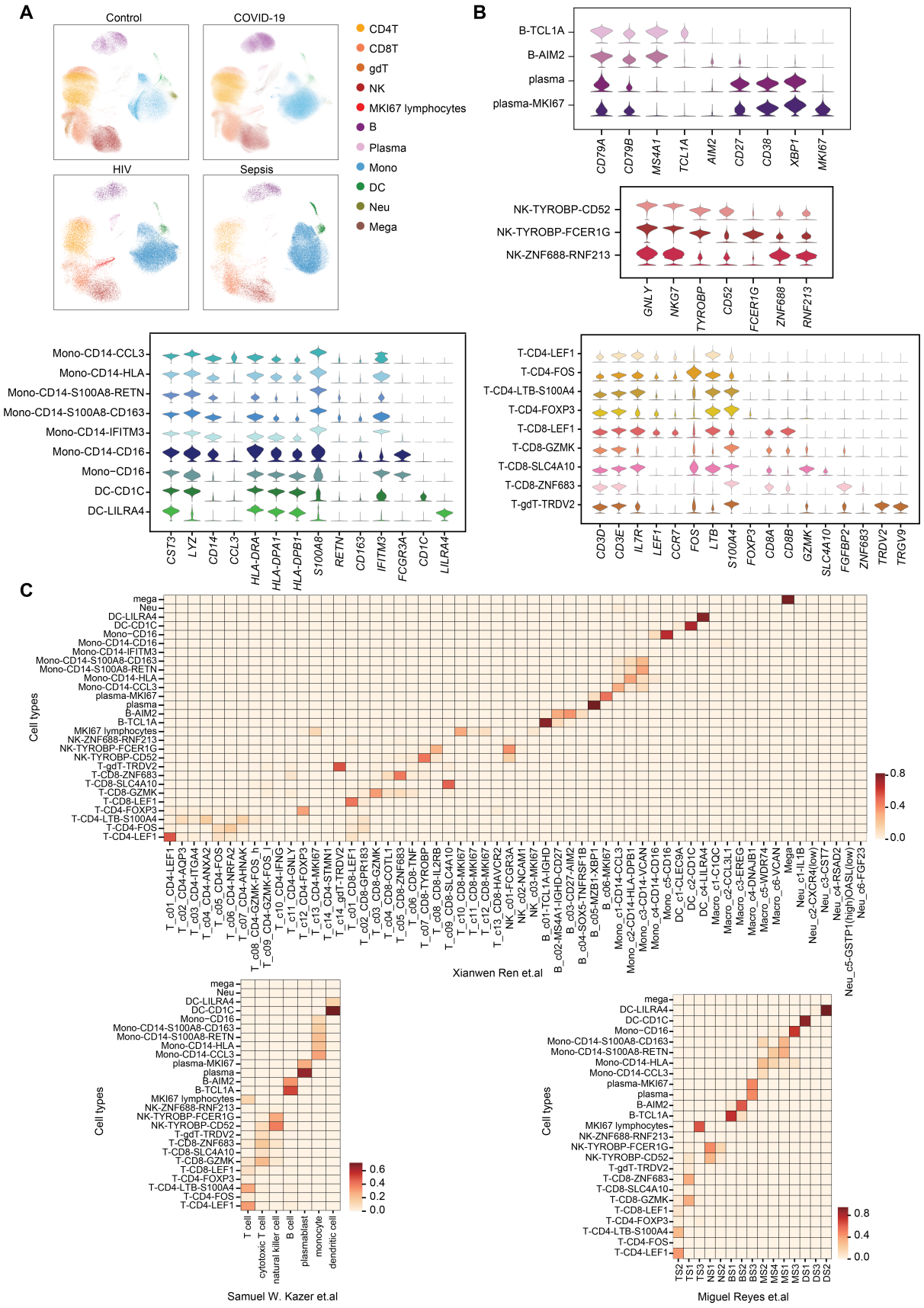

Figure S1. Identification of subtypes of integrated atlas of PBMCs from COVID-19, sepsis, and HIV infection patients. Related to Figure 1.

(A) UMAP projections showing cells from different diseases or healthy donors (Control, COVID-19, sepsis, HIV). (B) Violin plots of markers (columns) for subtypes (rows) in B cells, NK cells, myeloid cells, T cells. Violin plots are colored by subtypes. (C) Jaccard similarities between the subtypes and cell-type annotations in original studies. Mono, monocytes. DC, dendritic cells. Neu, neutrophils. Mega, megakaryocytes.

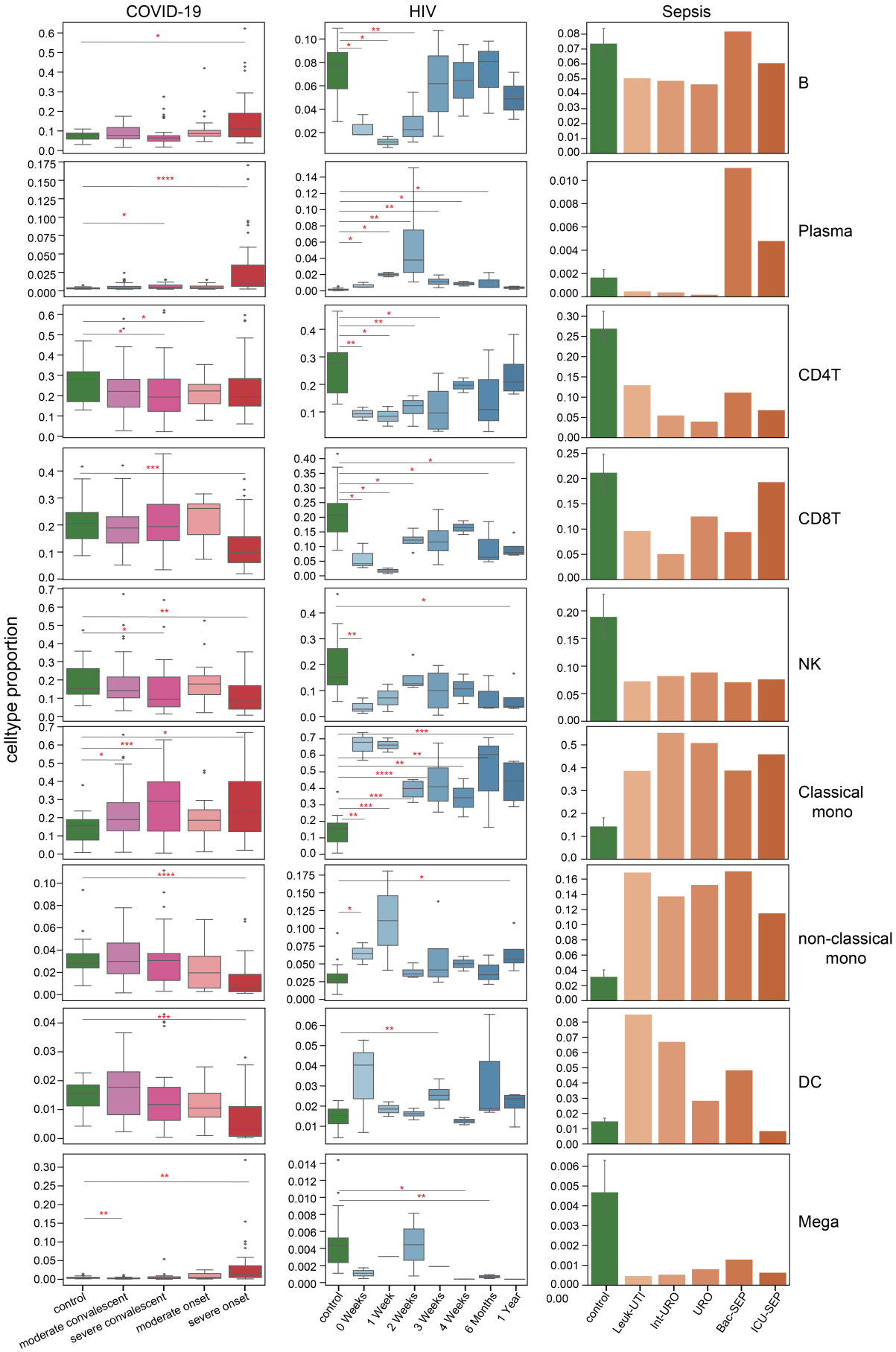
COVID-19
HIV
Sepsis
B
Plasma
CD4T
CD8T
NK
Classical mono
non-classical mono
DC
Mega
celltype proportion
control
moderate convalescent
severe convalescent
moderate onset
severe onset
0 Weeks
1 Week
2 Weeks
3 Weeks
4 Weeks
6 Months
1 Year
Leuk-UTI
Int-URO
URO
Bac-SEP
ICU-SEP

Figure S2. Compositional shifts of major subtypes of integrated atlas of PBMCs from COVID-19, sepsis, and HIV infection patients. Related to Figure 1.

Box plots of the proportion of cell subtypes of samples in different states from COVID-19, HIV infection (left and middle panel) compared to healthy donors. Bar plots of the proportion of subtypes from sepsis cohort in different states (right) compared to healthy donors. Boxes and bars are colored according to disease states. Samples with less than 1000 cells were filtered out (control, n=20; COVID-19: moderate convalescent, n=48, severe convalescent, n=35, moderate onset, n=18, severe onset, n=38; HIV, 0 Weeks, n=3, 1 Week, n=2, 2 Weeks, n=4, 3 Weeks, n=4, 4 Weeks, n=2, 6 Months, n=3, 1 Year, n=4). Statistical significance between disease states and healthy donors was evaluated with Wilcoxon rank-sum test (two-tailed). The mean and interquartile range (IQR), with whiskers extending to 1.5×IQR are shown in box plots. **** $P < 0.0001$, *** $P < 0.001$, ** $P < 0.01$, * $P < 0.05$.

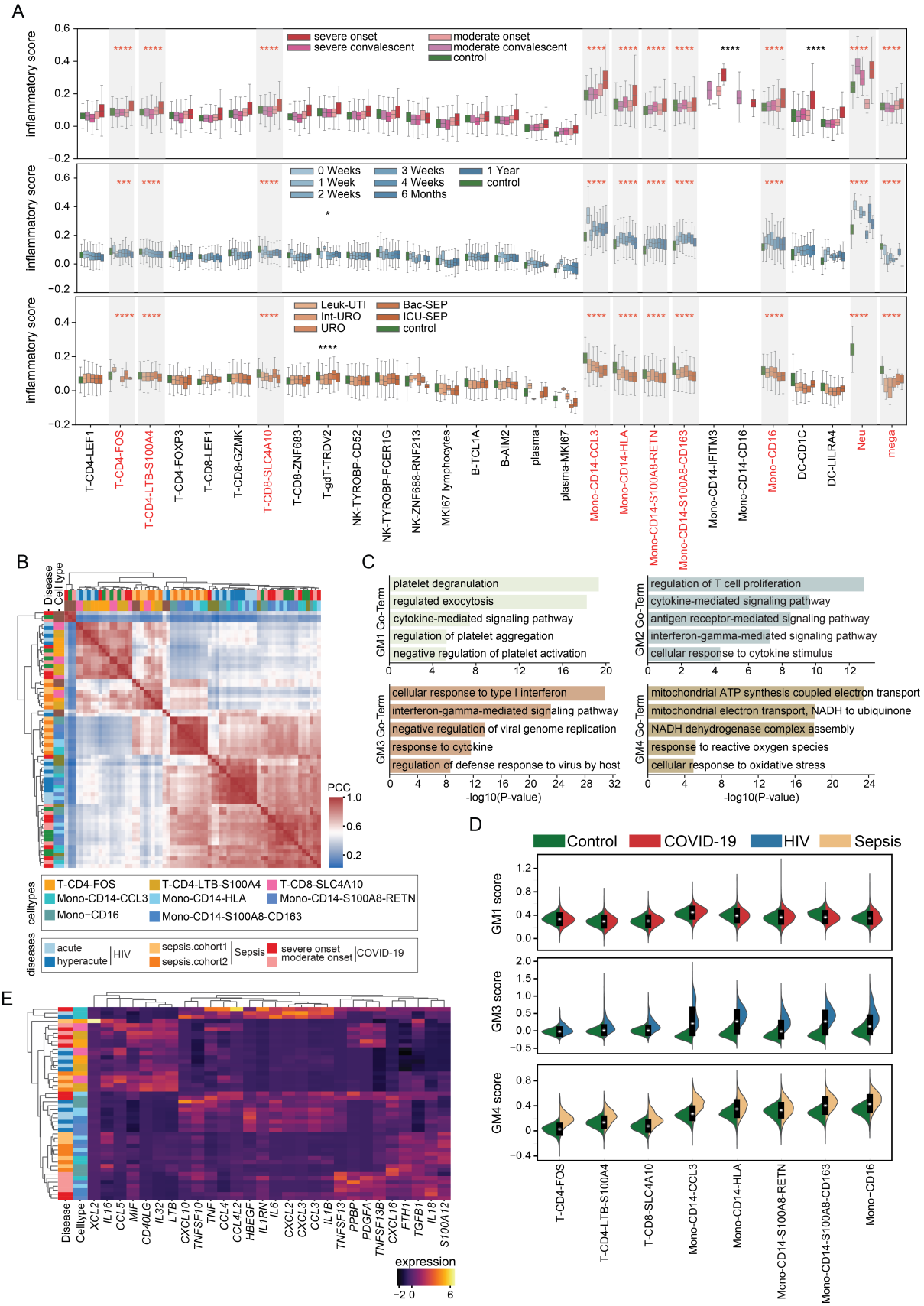
A
inflammatory score
severe onset
severe convalescent
moderate onset
moderate convalescent
control
0 Weeks
1 Week
2 Weeks
3 Weeks
4 Weeks
6 Months
1 Year
control
Leuk-UTI
Int-URO
URO
Bac-SEP
ICU-SEP
control
T-CD4-LEF1
T-CD4-FOS
T-CD4-LTB-S100A4
T-CD4-FOXP3
T-CD8-LEF1
T-CD8-GZMK
T-CD8-SLC4A10
T-CD8-ZNF683
T-gdT-TRDV2
NK-TYROBP-CD52
NK-TYROBP-FCER1G
NK-ZNF688-RNF213
MKI67 lymphocytes
B-TCL1A
B-AIM2
plasma
plasma-MKI67
Mono-CD14-CCL3
Mono-CD14-HLA
Mono-CD14-S100A8-RETN
Mono-CD14-S100A8-CD163
Mono-CD14-IFITM3
Mono-CD14-CD16
Mono−CD16
DC-CD1C
DC-LILRA4
Neu
mega
B
Disease
Cell type
PCC
celltypes
T-CD4-FOS
T-CD4-LTB-S100A4
T-CD8-SLC4A10
Mono-CD14-CCL3
Mono-CD14-HLA
Mono-CD14-S100A8-RETN
Mono−CD16
Mono-CD14-S100A8-CD163
diseases
acute
hyperacute
HIV
sepsis.cohort1
sepsis.cohort2
Sepsis
severe onset
moderate onset
COVID-19
C
GM1 Go-Term
platelet degranulation
regulated exocytosis
cytokine-mediated signaling pathway
regulation of platelet aggregation
negative regulation of platelet activation
GM2 Go-Term
regulation of T cell proliferation
cytokine-mediated signaling pathway
antigen receptor-mediated signaling pathway
interferon-gamma-mediated signaling pathway
cellular response to cytokine stimulus
GM3 Go-Term
cellular response to type I interferon
interferon-gamma-mediated signaling pathway
negative regulation of viral genome replication
response to cytokine
regulation of defense response to virus by host
GM4 Go-Term
mitochondrial ATP synthesis coupled electron transport
mitochondrial electron transport, NADH to ubiquinone
NADH dehydrogenase complex assembly
response to reactive oxygen species
cellular response to oxidative stress
-log10(P-value)
D
Control
COVID-19
HIV
Sepsis
GM1 score
GM3 score
GM4 score
T-CD4-FOS
T-CD4-LTB-S100A4
T-CD8-SLC4A10
Mono-CD14-CCL3
Mono-CD14-HLA
Mono-CD14-S100A8-RETN
Mono-CD14-S100A8-CD163
Mono−CD16
E
Disease
Celltype
XCL2
IL16
CCL5
MIF
CD40LG
IL32
LTB
CXCL10
TNFSF10
TNF
CCL4
CCL4L2
HBEGF
IL1RN
IL6
CXCL2
CXCL3
CCL3
IL1B
TNFSF13
PPBP
PDGFA
TNFSF13B
CXCL16
FTH1
TGFB1
IL18
S100A12
expression

Figure S3. Characterization of hyper-inflammatory cell subsets and inflammatory signatures. Related to Figure 2.

(A) Boxplots of the inflammatory score of cell subtypes in COVID-19, sepsis, and HIV infection. Statistical significance was evaluated with Mann-Whitney rank tests for each subtype versus all the other subtypes. The mean and interquartile range (IQR), with whiskers extending to 1.5×IQR are shown in box plots. **** P-value < 0.0001. (B) Unsupervised hierarchical clustering of the pearson correlation coefficients on normalized gene expression of hyper-inflammatory cell subsets in COVID-19, sepsis, and HIV infection. Color bars of the heatmap indicate the cell type and disease states (see legend for key). (C) Bar plots of representative biological pathways in gene modules (GM1, GM2, GM3, GM4) defined by WGCNA analysis. (D) Violin plot of module score (from left to right: GM1, GM3, GM4) among the hyperinflammatory cell subtypes in COVID-19, sepsis, HIV infection and healthy donors. (E) Unsupervised hierarchical clustering of normalized gene expression of cytokines for these three infectious diseases. Color bars on the left side indicate the cell subsets and disease states (see legend for key). In (A), (B), (E), Mono, monocytes. DC, dendritic cells. Neu, neutrophils. Mega, megakaryocytes.

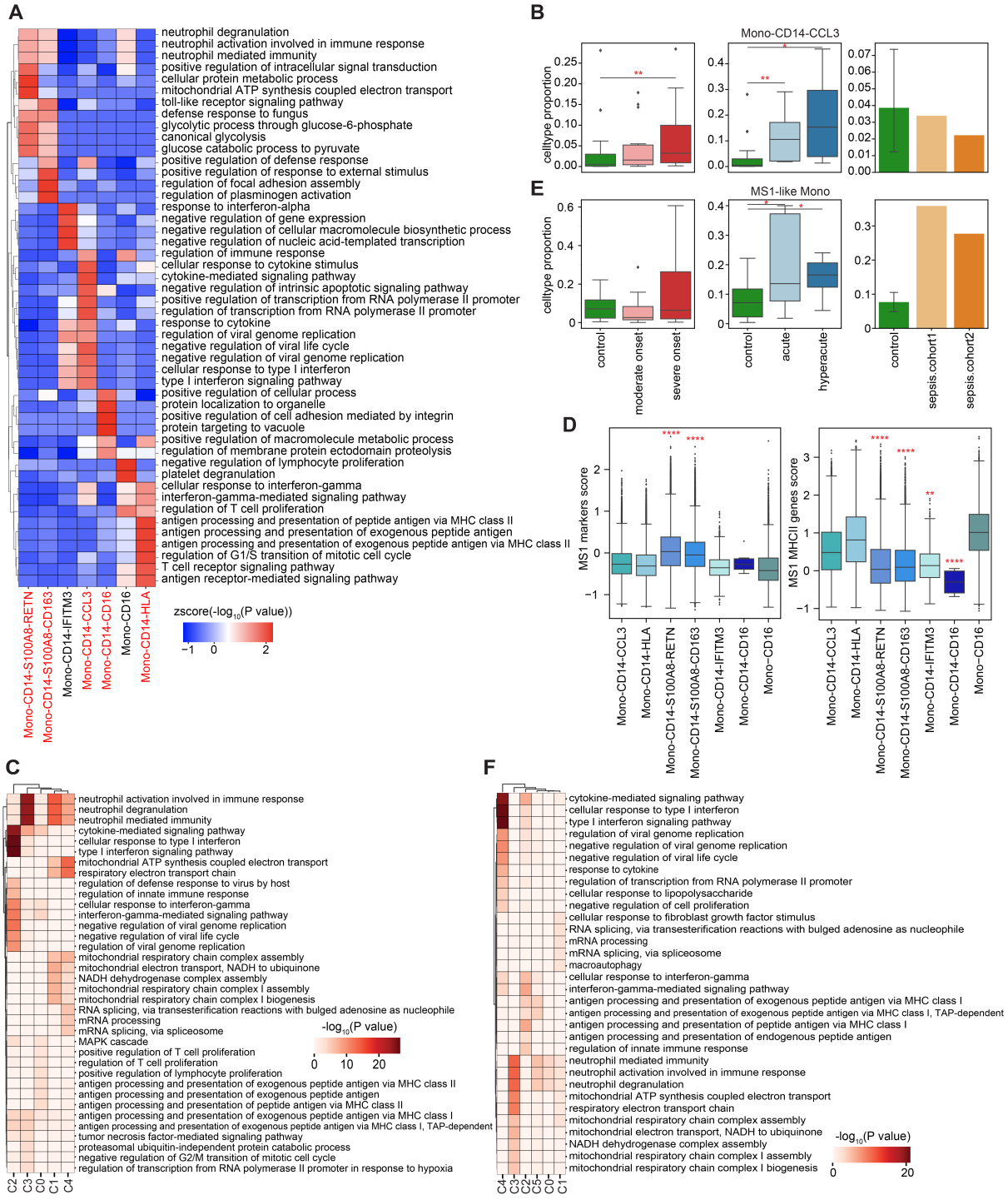

Figure S4. Functional characteristics of the monocyte subtypes. Related to Figure 3.

(A) Heatmap of top 10 enriched biological pathways using top 100 DEGs of each monocyte subtype. The subtype in red color denote the hyper-inflammatory cell subsets in monocytes. (B, E) Box plots of the cell proportion of Mono-CD14-CCL3 (B) and MS1-like monocytes (E) of samples in different states from COVID-19, sepsis, and HIV infection. (C, F) Unsupervised

hierarchical clustering showing biological pathways of gene clusters in Mono-CD14-CCL3 (C) and MS1-like monocytes (F). Filtering threshold: P-value < 0.01. (D) Box plots of the score of top 6 markers (RETN, CD63, ALOX5AP, SEC61G, TXN, and MT1X) of MS1 monocytes (left) and MHC II molecule score (right) in each monocyte subtype. Significance was evaluated with Mann-Whitney rank test (one-sided test, left: greater; right: less) for each subtype versus all the other subtypes.

MS1-like monocytes include Mono-CD14-S100A8-RETN and Mono-CD14-S100A8-CD163 subtypes. In (B) and (E), samples less than 1000 cells were removed before the cell proportion analysis (control, n=20; COVID-19, moderate onset, n=18, severe onset, n=38; HIV, acute, n=9, hyperacute, n=6). statistical significance was calculated by Kruskal-Wallis H-test. In (B), (D), (E), the mean and interquartile range (IQR), with whiskers extending to 1.5×IQR are shown in box plots. **** $P < 0.0001$, *** $P < 0.001$, ** $P < 0.01$, * $P < 0.05$.

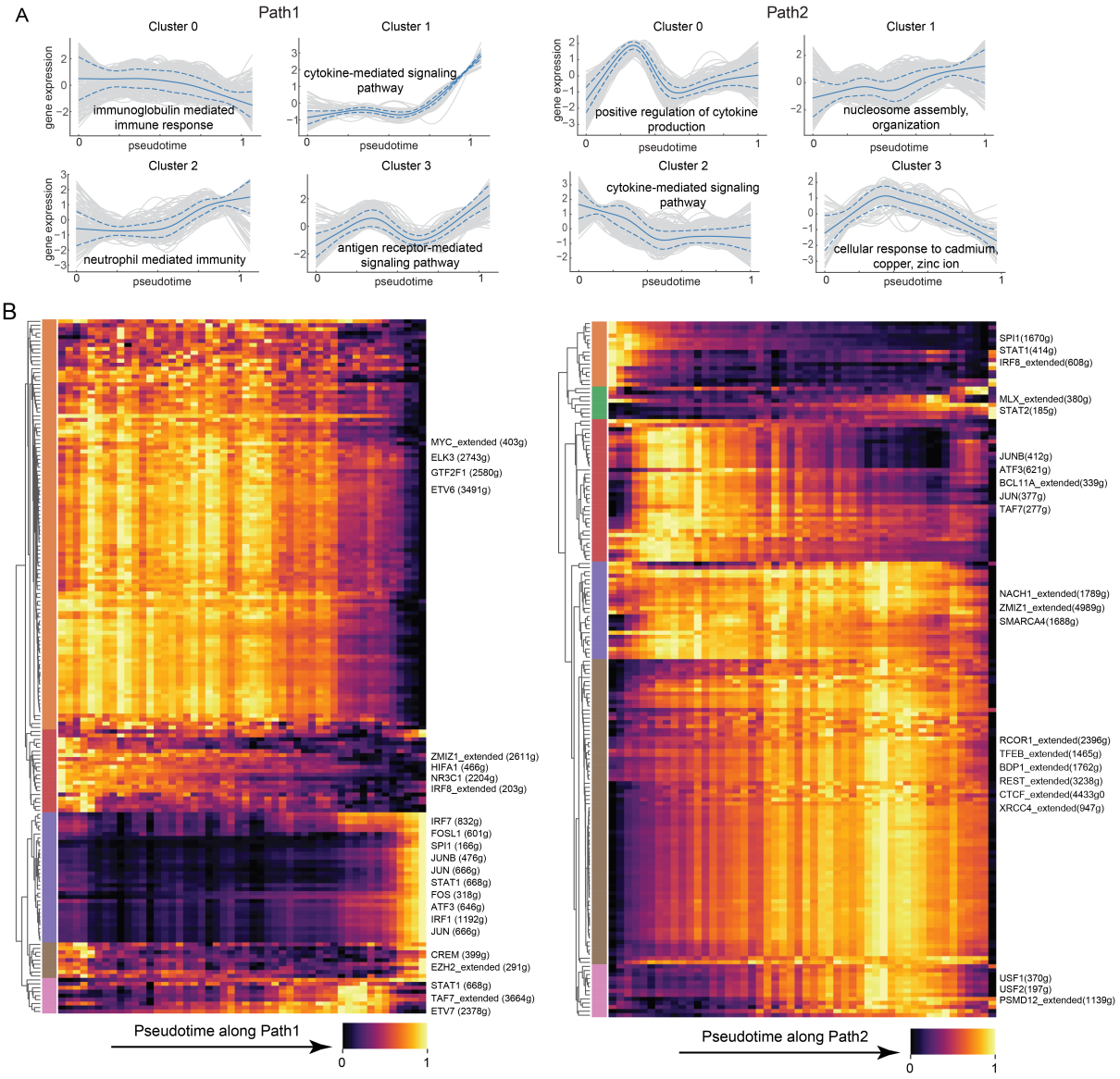

Figure S5. The dynamics of gene expression and regulators during the trajectory of monocytes. Related Figure 3.

(A) Plots showing cluster results of expression trends of top 1000 variable genes in Path1 (left) and Path2 (right). Solid blue line, mean expression trend of the cluster; Grey line, expression trend of a specific gene; Dotted blues lines, standard deviation. Each cluster panel is annotated with enriched gene ontology terms. (B) Heatmaps of the area under the curve (AUC) scores of transcription factors (TFs) in Path1 (left) and Path2 (right), as estimated by SCENIC. Cells were ordered along with the continuous pseudotime of Path 1 and Path 2, which were divided into 50 bins uniformly for visualization.

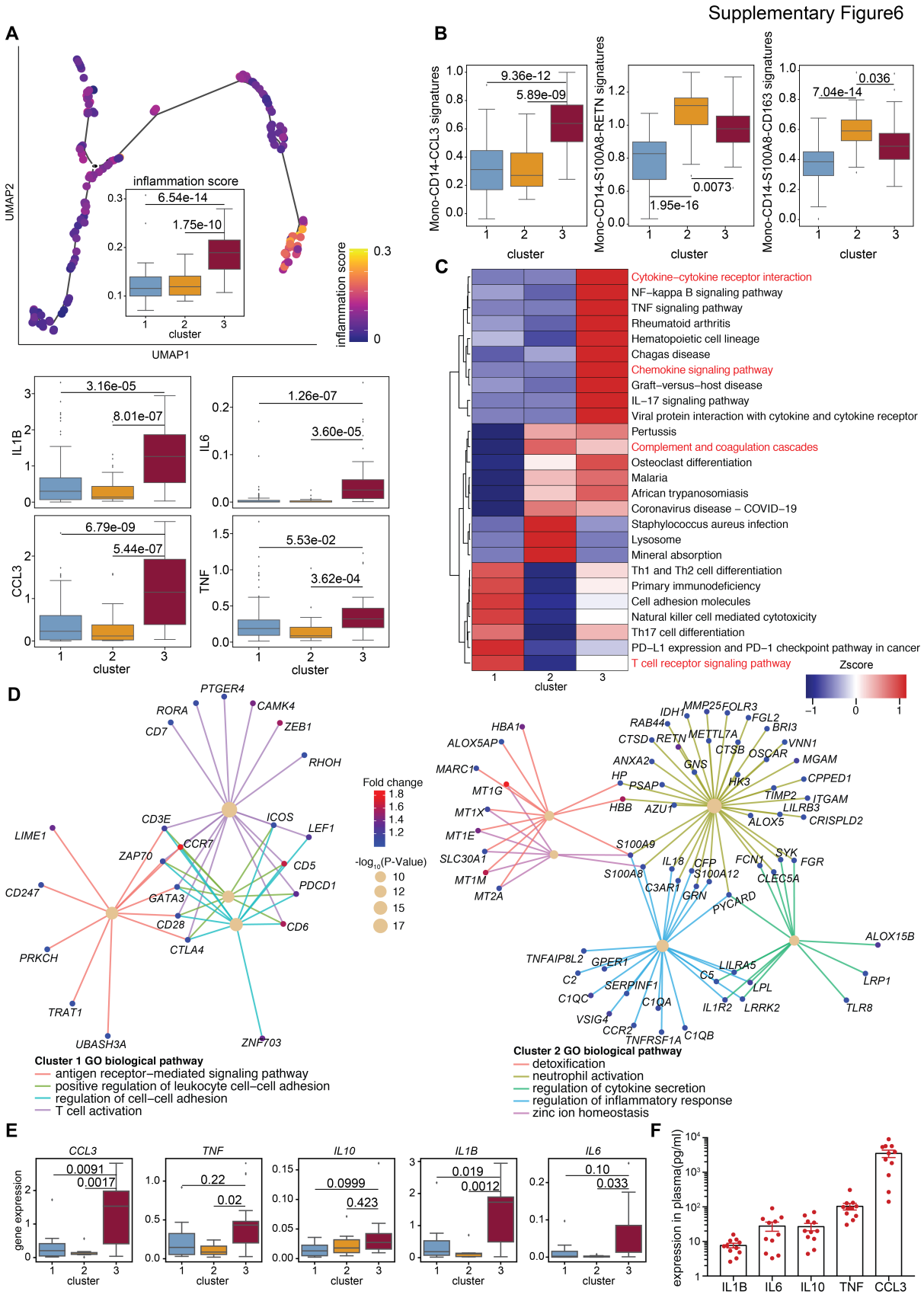

Figure S6. Differences of the three clusters in COVID-19 patients. Related to Figure 4.

(A) Top, UMAP embedding of samples of COVID-19 patients colored by inflammatory score. Box plot within the top panel statistically shows the inflammatory score in three clusters. Bottom, box plots of gene expression levels of IL1B, IL6, CCL3, and TNF in three clusters. (B) Box plots of signature scores (top 100 marker genes) for each subtype (from left to right, Mono-CD14-CCL3, Mono-CD14-S100A8-RETN, and Mono-CD14-S100A8-CD163) in three clusters. (C) Unsupervised hierarchical clustering of top-10 ranking KEGG pathways enriched by cluster-specific DEGs, the color bar indicates the z-score of -log10(P-value). (D) The diagram of biological pathways and genes enriched in samples of cluster 1 (left) and cluster 2 (right) from severe onset patients. Network edges represent gene-pathway associations, and edges of different pathways are indicated by different colors. The significance of the pathways was shown by circle size. The color bar from blue to red represents the fold change of gene expression level. P values were assessed by clusterProfiler's built-in function "enrichGO" with default parameters. (E) Box plots of gene expression of CCL3, TNF, IL10, IL1B, and IL6 of samples in three clusters from severe onset patients. (F) Bar plots showing cytokine concentration in the plasma of IL1B, IL6, IL10, TNF, and CCL3 of eleven matched patients in cluster3. All points are shown and bars represent mean with standard error of the mean (SEM).

In panel (A), (B), and (E), statistical significance was evaluated with Student t-test. The mean and interquartile range (IQR), with whiskers extending to 1.5×IQR are shown in box plots.

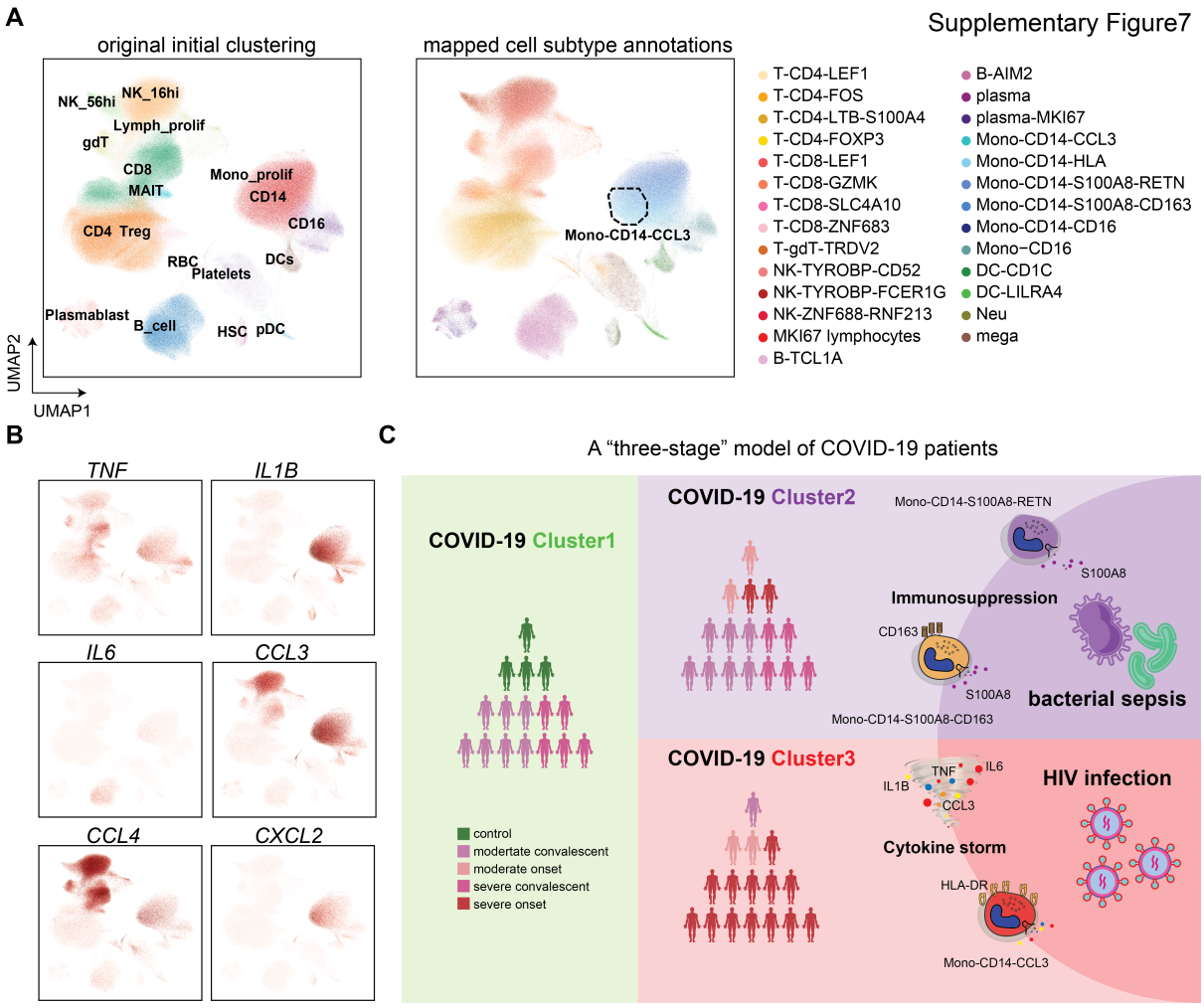

Figure S7. Independent large cohort analysis and schematic for our “three-stage” model. Related to Figure 4.

(A) UMAP embeddings of cell subtype annotations of the original study (Stephenson et al., 2021) (left) and mapped annotations based on the cell subtype annotation of the present study (right, label mapping performed using the ingest utilities in scanpy). (B) UMAP embeddings of cells colored by gene expression of pro-inflammatory cytokines (TNF, IL6, IL1B, CCL3, CCL4 and CXCL2). (C) Schematic for our “three-stage” model of COVID-19 patients representing the differences of inflammatory responses. Patients in stage 1 showed enrichment of T-CD4-LTB-S100A4 subtype, which support adaptive immune response to infection. Patients in stage 2 showed enrichment of two MS1-like monocyte subtypes, appearing to share immunosuppressive phenotypes with sepsis patients. COVID-19 patients in stage 3 shared

excessive inflammatory phenotypes (cytokine storm) with HIV patients.